A Comparison of Point Target Spectrum Derived for Multi-Aperture SAS

Haoran Wu*, Jinsong Tang and Yishuo Tong

Naval University of Engineering, Wuhan 430033, China

*Corresponding author e-mail: 13260539614@126.com

Abstract. Synthetic aperture sonar has an important application prospect in ocean resources exploration. The SAS receiver antennas generally have multi-aperture configuration, which lead that it is more difficult to obtain the analytical solution of the two-dimensional spectrum. In this paper, the analytical solutions of the multi-aperture SAS with two methods of displaced phase centre antenna (DPCA) and four-order the method of series reversion (MSR) are given respectively, and the phase errors and the imaging results of the two methods under the same conditions are compared by computer simulation. The results of the computer simulation show that MSR has a smaller phase error than the DPCA at the same squint angle, and the DPCA and MSR methods have the same image quality in the small squint angle, but the quality of MSR is much better than that of DPCA in the medium squint angle.

1. Introduction

Synthetic aperture sonar (SAS), originally designed for offshore oil and gas industry application, can be readily applied to scientific seafloor mapping [1]. SAS achieves high azimuth resolution by using small antenna of uniform linear motion to synthesize a large aperture [2]. The factors of ocean currents and asymmetric platforms may lead to squint phenomenon appearing.

SAS is difference with the radar signal model because the azimuth frequency and the range time cannot be blurred simultaneously for the low speed of sound in water. To solve this contradiction, the SAS receiver antennas generally have multi-aperture configuration [3-5]. However, the multi-aperture configuration lead that the two-dimensional spectrum for SAS become more complex and difficult. So far, there are many methods to get the two-dimensional spectrum, in which DPCA and MSR are the two common methods. In DPCA, the double root range history is approximated into the monocratic range history, then the expression of the two-dimensional spectrum can been obtained by learning from the monocratic radar [6]. MSR is a general method, that the double root range history is approximated by the expression of taylor series and the expression of the two-dimensional spectrum can been obtain by using series reversion. The accuracy of this method is “scalable” in the sense that its accuracy depends on the number of the terms used in the power series [7].

In addition, since the azimuth walking during the transmission and reception of SAS sonar cannot be neglected, the expression of the exact range history is very complicated and cannot be directly used for imaging processing. DPCA can only consider the non-aperture-dependent azimuth walking during the transmission and reception, which leads to a larger phase errors when the squint angle is not small. However, MSR directly process the exact range history and can handle the case that the azimuth

walking during the transmission and reception is aperture-dependent, so this method can be used in the synthetic aperture system with a greater squint angle and longer aperture.

This article is organized as follows. Section II presents derivation of the two-dimensional spectrum which include the squint multi-aperture SAS signal model, the two-dimensional spectrum based on DPCA and the two-dimensional spectrum based on MSR. In Section III, some simulations are performed. In Section IV, some comments are given.

2. Derivation of the Two-dimensional Spectrum

2.1. The Squint Multi-aperture SAS Signal Model

After demodulation to baseband, the received signal of the i th receiver comes from the point target P, which is expressed as.

$$ss_i(\tau,t;r)=p\left(\tau-\frac{R_i\ (t;r)}{c}\right)\cdot\omega_a(t)\cdot\exp\left\{j\pi k\left(\tau-\frac{R_i\ (t;r)}{c}\right)^2\right\}\cdot\exp\left\{-j\frac{2\pi f_0}{c}R_i\ (t;r)\right\} \tag{1}$$

where τ is the fast time, t is the slow time, $p(\mathrm{g})$ is the pulse envelope, $\omega_a(\mathrm{g})$ is the antenna weighting, k is the FM rate, c is the speed of sound, f_0 is the carrier frequency, $R_i(t;r)$ is the instantaneous slant range, r is the slant range between the transmitter and the point target at the beam center crossing time. According to the reference [8], the accuracy range history $R_i(t;r)$ is formulated as follows:

$$R_i(t;r)=\sqrt{r^2-2vtr\sin\theta_{sq}+v^2t^2}+\sqrt{r^2+d_i^2-2v\left(t+t_i^*\right)\left(r\sin\theta_{sq}-d_i\cos\theta_{yaw}\right)+v^2\left(t+t_i^*\right)^2} \tag{2}$$

$$\begin{aligned}t_i^*(t;r)=&\frac{1}{c^2-v^2}\left[v^2t-vr\sin\theta_{sq}+vd_i\cos\theta_{yaw}+c\sqrt{r^2+v^2t^2-2vtr\sin\theta_{sq}}\right]\\&+\frac{1}{c^2-v^2}\sqrt{\left(v^2t-vr\sin\theta_{sq}+vd_i\cos\theta_{yaw}+c\sqrt{r^2+v^2t^2-2vtr\sin\theta_{sq}}\right)^2+\left(1+2vt\cos\theta_{yaw}\right)d_i^2\left(c^2-v^2\right)}\end{aligned} \tag{3}$$

Where v is the platform velocity and d_i is the baseline between the transmitter and the i th aperture, θ_{sq} is the squint angle, θ_{yaw} is the yaw angle.

2.2. The Two-dimensional Spectrum Based on DPCA

According to DPCA [9], the exact range history $R_i(t;r)$ can been approximated by

$$R_i(t;r)\approx 2\sqrt{r^2-2vr\sin\theta_{sq}\left(t+\frac{r}{c}+\frac{d_i}{2v\cos\theta_{yaw}}\right)+v^2\left(t+\frac{r}{c}+\frac{d_i}{2v\cos\theta_{yaw}}\right)^2}+\left[\frac{v^2}{4r}\left(\frac{2r}{c}+\frac{d_i}{v\cos\left(\theta_{yaw}\right)}\right)^2+\frac{d_i\sin\left(\theta_{sq}\right)}{\cos\left(\theta_{yaw}\right)}\right] \tag{4}$$

By using the stationary phase principle (POSP) [10], the range Fourier transform and the azimuth Fourier transform for (1) is carried out, and the two-dimensional frequency domain expression of the point target signal is given by

$$\begin{aligned}SS(f_r,f_a;r)=&P(f_r)W_a(f_a-f_{dc})\exp\left\{-j\frac{\pi f_r^2}{k}\right\}\exp\left\{-j\frac{4\pi(f_0+f_r)}{c}\left[\frac{v^2}{4r}\left(\frac{2r}{c}+\frac{d_i}{v\cos\left(\theta_{yaw}\right)}\right)^2+\frac{d_i\sin\left(\theta_{sq}\right)}{\cos\left(\theta_{yaw}\right)}\right]\right\}\\&\times\exp\left\{j\frac{2\pi f_a}{c}\left(\frac{r}{c}+\frac{d_i}{2v\cos\theta_{yaw}}-\frac{r\sin\theta_{sq}}{v}\right)\right\}\exp\left\{-j\frac{4\pi f_0 r\cos\theta_{sq}}{c}\sqrt{1-\frac{c^2f_a^2}{4v^2f_0^2}+\frac{2f_r}{f_0}+\frac{f_r^2}{f_0^2}}\right\}\end{aligned} \tag{5}$$

Where f_a is the azimuth frequency, f_r is the range frequency, $P(f_r)$ is the range spectrum envelope, $W_a(f_a)$ is the azimuth spectrum envelope, f_{dc} is the Doppler center frequency.

2.3. The Two-dimensional Spectrum Based on MSR

MSR [11] is the most widely used one and its most prominent feature is that the accuracy of the spectrum is only controlled by the number of terms in the expansion of Taylor series for the accuracy range history. According to the exact delay history $t_i^*(t;r)$ (3), the exact range history can been obtained by

$$R_i(t;r) = ct_i^*(t;r) \tag{6}$$

By expanding into a power series of t, and keeping terms up to t^4, $R_i(t;r)$ become

$$R_i(t;r) \approx k_0 + k_1 t + k_2 t^2 + k_3 t^3 + k_4 t^4 \tag{7}$$

Where

$$k_0 = \frac{c}{c^2 - v^2}\left(cr - vr\sin\theta_{sq} - vd_i\cos\theta_{yaw} + T\right) \tag{8}$$

$$k_1 = -\frac{c}{2\left(c^2 - v^2\right)rT}\left(2cvrT\sin\theta_{sq} - 2rv^2T - U\right) \tag{9}$$

$$k_2 = \frac{c}{8\left(c^2 - v^2\right)T^3r^3}\left(4cr^2v^2T^3\cos^2\theta_{sq} + 4PT^2 - U^2r\right) \tag{10}$$

$$k_3 = \frac{c}{16\left(c^2 - v^2\right)r^5T^5}\left(8cv^3r^3T^5\sin\theta_{sq}\cos^2\theta_{sq} + 8GT^4 - 4PT^2Ur + U^3r^2\right) \tag{11}$$

$$\begin{aligned} k_4 = {} & \frac{c}{128\left(c^2 - v^2\right)r^7T^7}\left(20cr^4v^4T^7\sin^2 2\theta_{sq} - 16cr^4v^4T^7\cos^2\theta_{sq} + 16FT^6cv^5\right) \\ & + \frac{c}{128\left(c^2 - v^2\right)r^7T^7}\left(24PT^2U^2r^2 - 32GT^4Ur - 16P^2T^4r - 5U^4r^3\right) \end{aligned} \tag{12}$$

Where

$$T = \sqrt{\left(c - v\sin\theta_{sq}\right)^2 r^2 + \left(c^2 - v^2\right)d_i^2 + 2crvd_i\cos\theta_{yaw}} \tag{13}$$

$$U = 2vr\left(c - v\sin\theta_{sq}\right)\left(rv - cr\sin\theta_{sq} + cd_i\cos\theta_{yaw}\right) \tag{14}$$

$$G = cv^4r^2\sin^2\theta_{sq}\left(rd_i\sin\theta_{sq}\cos\theta_{yaw} + r^2\cos^2\theta_{sq}\right) \tag{15}$$

$$P = v^2\left(c^2r^3 + r^3v^2 + cvr^3\sin^3\theta_{sq} - 3cvr^3\sin\theta_{sq} + cvd_ir^2\cos^2\theta_{sq}\cos\theta_{yaw}\right) \tag{16}$$

$$F = r^2 \cos^2\theta_{sq}\left(5r^3 \sin\theta_{sq}\cos^2\theta_{sq} + 5d_i r^2 \cos\theta_{yaw}\sin^2\theta_{sq} - r^2 d_i \cos\theta_{yaw}\right) \quad (17)$$

Using the Neo's method [11], the two-dimensional spectrum for a point target can be obtained.

$$SS_{MSR}(f_r, f_a; r) = P(f_r)W_a\left(f_a + (f_o + f_r)\frac{k_1}{c}\right)\exp\left\{j\phi(f_r, f_a; r)\right\} \quad (18)$$

Where $\phi(f_r, f_a; r)$ is the phase function.

$$\begin{aligned}\phi(f_r, f_a; r) = &-2\pi\left(\frac{f_o + f_r}{c}\right)k_0 + \frac{\pi f_r^2}{K} \\ &+2\pi\frac{c}{4k_2(f_o + f_r)}\left(f_a + (f_o + f_r)\frac{k_1}{c}\right)^2 \\ &+2\pi\frac{c^2 k_3}{8k_2^3(f_o + f_r)^2}\left(f_a + (f_o + f_r)\frac{k_1}{c}\right)^3 \\ &+2\pi\frac{c^3(9k_3^2 - 4k_2k_4)}{64k_2^5(f_o + f_r)^3}\left(f_a + (f_o + f_r)\frac{k_1}{c}\right)^4\end{aligned} \quad (19)$$

3. Simulation Results

In order to verify the validity of the spectrum in the paper, simulations are carried out in this section. The system parameters are listed in Table 1.

Table 1. SAS System Parameters.

Carrier frequency	Bandwidth	Pulse width	PRI	Antenna length(transmitter)	Antenna length(aperture)	Velocity	Aperture number
150kHz	10kHz	10ms	400ms	0.08m	0.04m	1.6m/s	32

To quantitatively measure the approximate accuracy of the exact range history, the range history error of wavelength normalization is obtained by the computer simulation under different squint angles and different approximating methods.

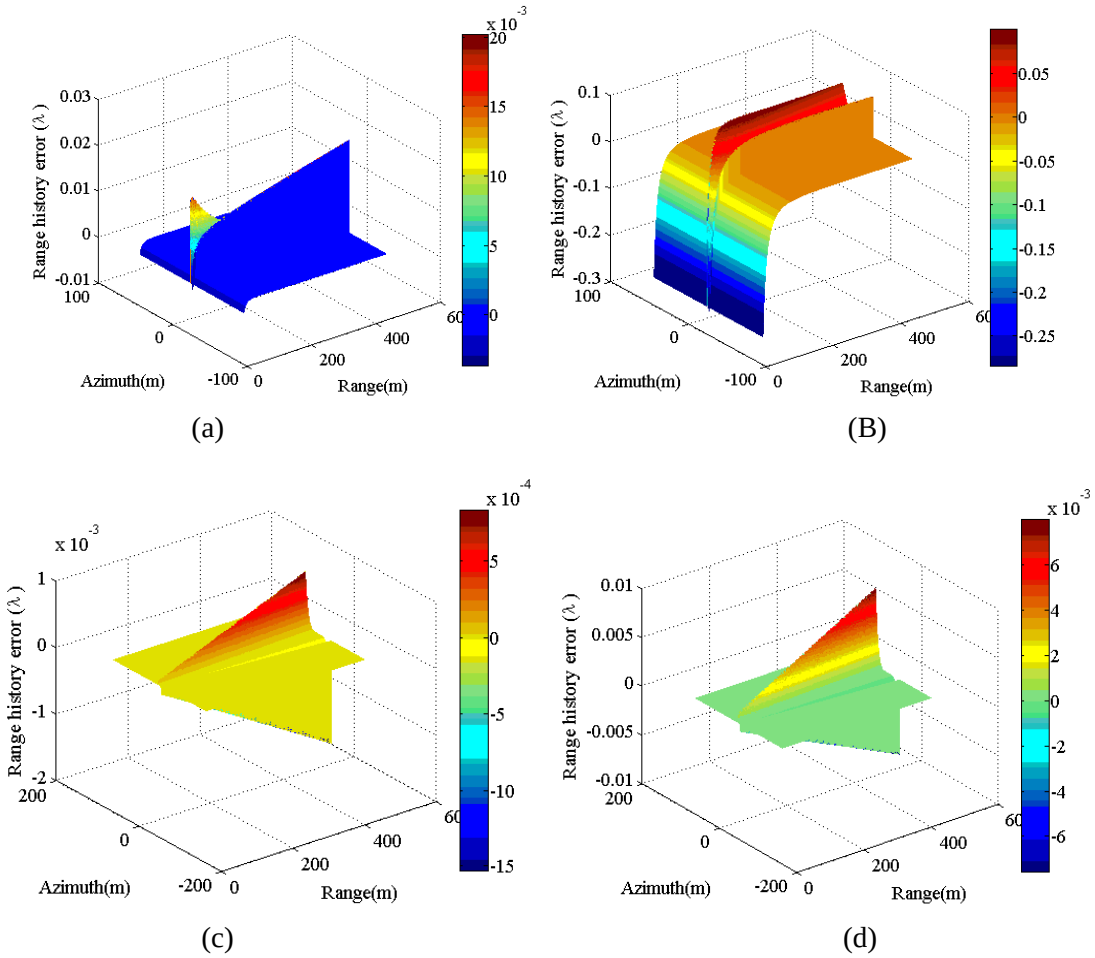

Figure 1. The sub images from left to right in each row correspond to the range history error of DPCA for 2^0 squint angle, the range history error of DPCA for 20^0 squint angle, the range history error of MSR for 2^0 squint angle, the range history error of MSR for 20^0 squint angle.

Fig 1 (a) and Fig (b) is the results of range history using DPCA when the squint angle is 2^0 and 20^0. Fig 1 (c) and Fig (d) is the results of range history using MSR when the squint angle is 2^0 and 20^0. The phase errors of Fig 1 (a), Fig 1 (b), Fig 1(c) and Fig 1 (d) are respectively 0.0238λ, 0.3848λ, 0.0024λ, 0.0156λ. The results of the phase error show that MSR has a smaller phase error than the DPCA at the same squint angle.

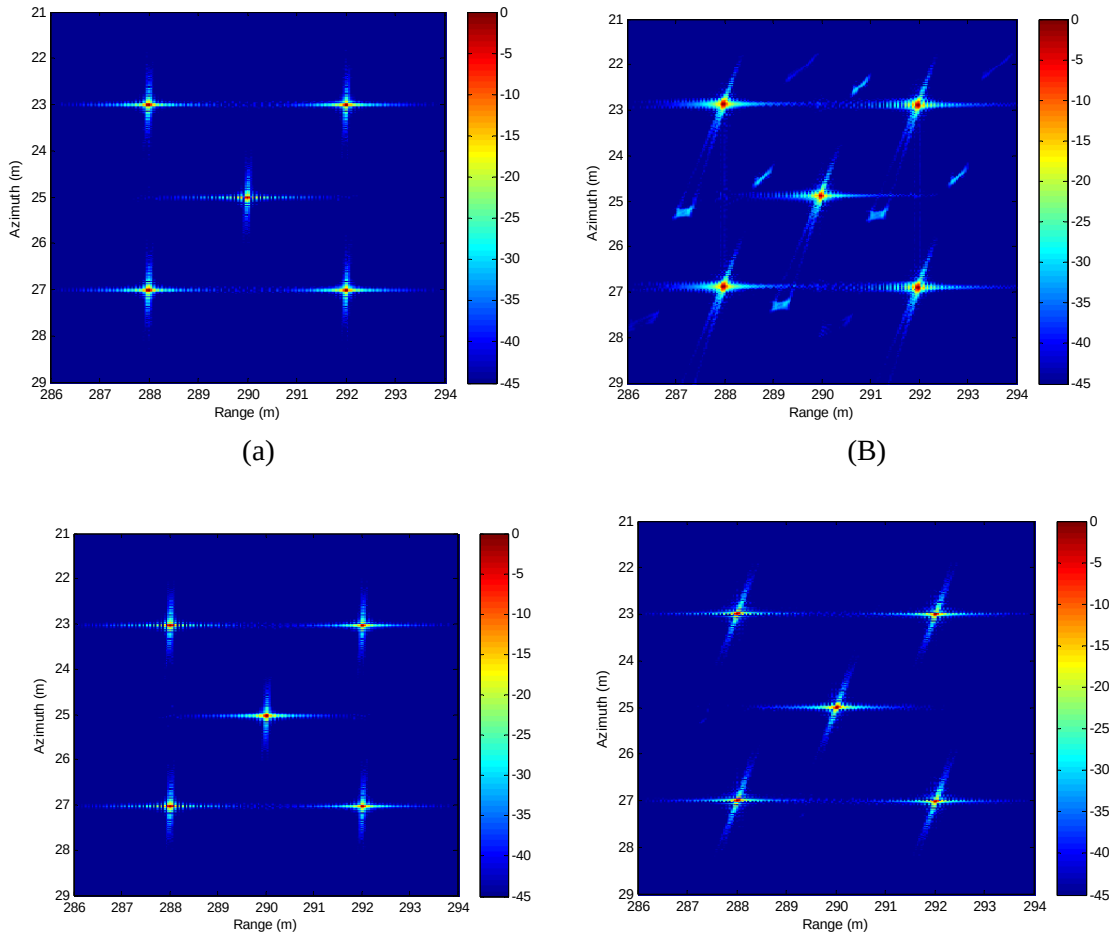

Figure 2. The sub images from left to right in each row correspond to the image of point scatter of DPCA for 2^0 squint angle, the image of point scatter of DPCA for 20^0 squint angle, the image of point scatter of MSR for 2^0 squint angle, the image of point scatter of MSR for 20^0 squint angle.

A simulation based on a flat earth model is presented. Five point target are used in the simulation. These point targets are illuminated at the same time. The separation between adjacent point targets is 2m in azimuth direction and is 2m in range.

Fig 2 (a) and Fig 2 (b) is the results of processing five simulated point using DPCA when the squint angle is 2^0 and 20^0. Fig 2 (c) and Fig 2 (d) is the results of processing five simulated point using MSR when the squint angle is 2^0 and 20^0. The results of Fig 2 (a), Fig 2 (b), Fig 2 (c) and Fig 2 (d) show that the DPCA and MSR methods have the same image quality in the small squint angle, but the quality of MSR is much better than that of DPCA in the medium squint angle.

4. Conclusion

In this paper, the analytical solutions of the multi-aperture SAS with two methods of DPCA and four-order MSR are compared, and the phase errors and the imaging results of the two methods under the same conditions are compared by computer simulation. The results of the computer simulation show that MSR has a smaller phase error than the DPCA at the same squint angle, and the DPCA and MSR methods have the same image quality in the small squint angle, but the quality of MSR is much better than that of DPCA in the medium squint angle.

Acknowledgments
This work was financially supported by the National Natural Science Foundation of China under Grant 61671461.

References

[1] Denny A, Hansen R E, Olsmo.S T and B.Pedersen R 2015 the use of synthetic aperture sonar to survey seafloor massive sulfide deposits *the journal of ocean technology* 10.
[2] Marx D, Nelson M, Chang E, Gillespie W, Putney A and Warman K 2000 An introduction to synthetic aperture sonar. In: *Proceedings of the Tenth IEEE Workshop on Statistical Signal and Array Processing (Cat. No.00TH8496)*, pp 717 - 21.
[3] Gilmour.G.A 1978 Synthetic Aperture Side-Looking Sonar System *Journal of the Acoustical Society of America* **65** 557 - 62.
[4] Putney A, Chang E, Chatham R, Marx D, Nelson M and Warman L K 2001 Synthetic aperture sonar-the modern method of underwater remote sensing. In: *2001 IEEE Aerospace Conference Proceedings (Cat. No.01TH8542)*, pp 4/1749-4/56 vol. 4.
[5] Douglas.B.L L H 1993 Synthetic-aperture sonar imaging with a multiple-element receiver array. In: *IEEE International Conference on Acoustics, Speech, and Signal Processing*, pp 445 – 8.
[6] Wu H, Tang J and Ma M 2017 Range Doppler algorithm of the Multi-Receiver SAS in the Squint Mode. In: *Underwater acoustics conference & exhibition*, (Skiathos. Greece pp 1049 - 58.
[7] Wu H, Tang J and Zhong H 2017 A new range doppler algorithm for processing squint multi-receiver SAS data. In: *10th International Congress on Image and Signal Processing, BioMedical Engineering and Informatics*, (Shanghai.China).
[8] Wu H, Tang J and Ma M 2017 Range Doppler algorithm of the multi-receiver SAS in the squint mode. In: *4th Underwater Acoustics Conference and Exhibition*, (Skiathos, Greece).
[9] Gebert N, Krieger G and Moreira A 2005 SAR signal reconstruction from non-uniform displaced phase centre sampling in the presence of perturbations. In: *Proceedings. 2005 IEEE International Geoscience and Remote Sensing Symposium, 2005. IGARSS '05.*, pp 1034 - 7.
[10] A. Papoulis 1977 *Signal Analysis* (New York: McGraw - Hill).
[11] Neo Y L, Wong F and Cumming I G 2007 A Two-Dimensional Spectrum for Bistatic SAR Processing Using Series Reversion *IEEE Geoscience and Remote Sensing Letters* **4** 93 - 6.